# Nano-Metals I. Effects of O2 Gas on the Size and Structure of Cr Clusters Formed by Plasma-Gas-Condensation

**Article** *in* MATERIALS TRANSACTIONS · August 2001

Impact Factor: 0.68 · DOI: 10.2320/matertrans.42.1480



**3 authors**, including:

T. Hihara
Nagoya Institute of Technology
**201** PUBLICATIONS **1,681** CITATIONS
SEE PROFILE

Dong-Liang Peng
Xiamen University
**178** PUBLICATIONS **2,046** CITATIONS
SEE PROFILE

*Materials Transactions*, Vol. 42, No. 8 (2001) pp. 1480 to 1484
Special Issue on Nano-Metals I


# Effects of $O_2$ Gas on the Size and Structure of Cr Clusters Formed by Plasma-Gas-Condensation

Takehiko Hihara, Dong-Liang Peng * and Kenji Sumiyama

*Department of Materials Science and Engineering, Nagoya Institute of Technology, Nagoya 466-8555, Japan*

Cr clusters have been produced by a plasma-gas-condensation type cluster deposition apparatus, and studied using a time-of-flight mass spectrometer and a transmission electron microscope. The Cr clusters formed in high pressure inert (Ar and/or He) gas atmosphere are of an A15-type structure. When an $O_2$ gas is mixed with the inert gases in the source (sputtering) chamber, a bcc phase is formed together with $Cr_2O_3$. The $O_2$ gas introduction leads to an increase in the gas temperature of the source chamber probably due to release of the formation enthalpy of the oxide. The A15 phase is annealed by such excess heat and becomes the equilibrium bcc phase. The sizes of bcc clusters are smaller than those of the A15-clusters, probably due to the heterogeneous nucleation promoted by the oxide formation.

(Received January 23, 2001; Accepted March 19, 2001)

***Keywords***: *A15-type structure, bcc structure, Chromium cluster, plasma-gas-condensation, time-of-flight mass spectrometer*

## 1. Introduction

Small clusters reveal unique physical and chemical properties, which are size dependent and quite different from those of their bulk counterparts.[1,2] Nanometer-size-clusters produced via vapor condensation[3–6] and chemical reactions[7,8] were used as building blocks to fabricate new type nano-structure-controlled materials, *i.e.*, cluster assembled materials.[9,10] For such cluster assembling,[11–13] we have developed a plasma-gas-condensation (PGC) type cluster deposition apparatus, which is similar to the one originally developed by Haberland *et al.*[5,6] This is a combination of sputter vaporization and inert gas condensation techniques, that enables one to vaporize refractory metals and to control the cluster size between 2 and 13 nm in diameter. We have investigated the cluster formation process in the PGC type cluster source and found that the cluster residence time in the source and the collision frequencies of metallic vapor atoms with inert gas atoms and with growing clusters are very important to control the cluster size and its distribution.[14,15]

Besides the cluster size control, the cluster structure control is highly desired. In this context, Cr clusters are interesting because an A15 type metastable phase has been reported in Cr fine particles produced with inert gas-condensation. Since its first finding by Kimoto *et al.*,[16] it has been obtained in films and fine particles produced by rapid quenching techniques such as sputtering, thermal evaporation and inert gas-condensation methods.[17–19] It transforms to the equilibrium bcc phase on thermal heating, where the transformation is exothermic.[20] The A15 phase has been also obtained in other VIa group metals, *i.e.*, Mo and W, whose equilibrium phases are of a bcc structure.[21]

The forming ability of the A-15 phase is very sensitive to the atmospheric conditions such as presence of an $O_2$ impurity and temperature.[16–19] In order to understand the formation process of A15-type and bcc Cr clusters, we measured both mass spectra of free clusters from the PGC cluster source and transmission electron microscope (TEM) images of deposited clusters. In particular, we studied effects of $O_2$ gas mixing with inert gases on the size and structure of Cr clusters.

## 2. Experiment

Cr clusters were synthesized by the PGC apparatus (see Fig. 1), whose details have been described elsewhere.[14,15] The metal vapors were generated from a Cr target by dc magnetron sputtering. A continuous Ar gas stream up to $4.5 \times 10^{-4}$ mol/s (1 mol/s = $1.34 \times 10^6$ sccm, standard cubic centimeter per minute) was adjusted by a fine mass flow controller and injected through a small gap of 0.3 mm between the target and the shield cover. Clusters nucleate in a high pressure Ar gas atmosphere (0.2–0.4 kPa) and grow in the space between the target and the nozzle (the growth region), whose length, $L_g$, can be varied by moving the sputtering source back and forth. A He gas stream up to $4.5 \times 10^{-4}$ mol/s and an $O_2$ gas stream up to $1.5 \times 10^{-6}$ mol/s were also introduced into the source (sputtering) chamber from a gas inlet located at the backside of the source. In the present experiment, we did not cool the PGC cluster source by liquid nitrogen. The cluster beam was extracted through the nozzle of 5 mm in diameter by a differential pumping system and further collimated by the three skimmers. The background pressure was $4 \times 10^{-7}$ Pa and the operational pressure during cluster deposition was $3 \times 10^{-5}$ Pa in the deposition chamber.

A time-of-flight mass spectrometer (TOF-MS)[15] has been designed in order to detect large clusters with wide mass range of 1–$10^7$ amu (1 amu = $1.66 \times 10^{-27}$ kg). The TOF-MS chamber was evacuated down to $5 \times 10^{-6}$ Pa by a turbo molecular pump. In the source chamber, a large amount of Cr clusters was ionized via a penning process,[5] because electrons excite Ar atoms to the metastable high energy state in the glow discharge region. The positively ionized clusters are extracted by the pulsed potential field, $E_1$, of 150 kV/m and further accelerated by the electric field, $E_2$, of 600 kV/m. After passing through the free flight zone of 0.2 m in length, the clusters were further accelerated by a static electric field of −700 kV/m, which was necessary to improve the detec-

*CREST, Japan Science and Technology Corporation (JST), Kawaguchi 332-0012, Japan.

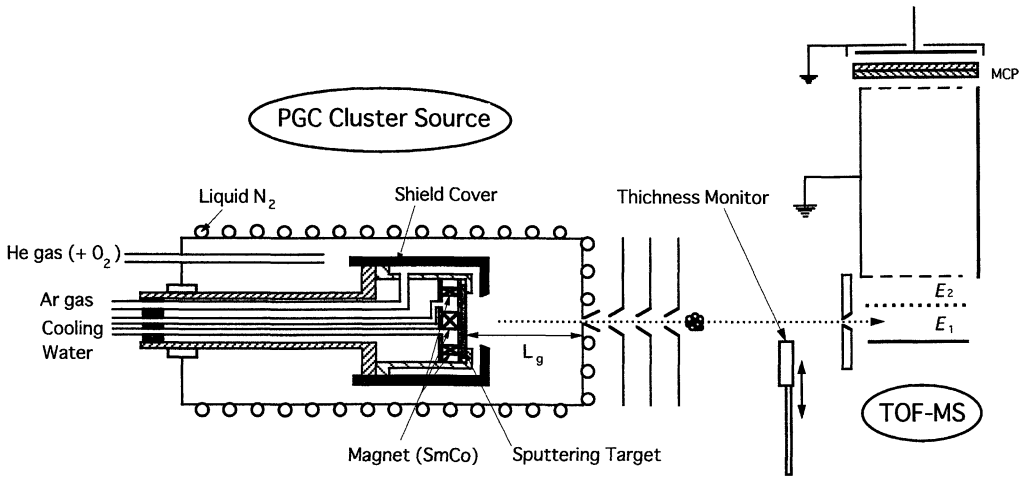


Fig. 1 Schematic drawing of the plasma-gas-condensation (PGC) type cluster deposition apparatus and the time-of-flight mass spectrometer for large cluster detection used in the present experiments.

tion efficiency of heavy clusters. The ion-signals detected by a multi-channel plates (MCP) were sent to a discriminator (Fast Comtec 7011) and accumulated by a multi-channel scaler (MCS) system (Fast Comtec 7885 MCD).

The deposition rate of Cr clusters was measured by a quartz oscillator-type thickness monitor installed behind the substrate. The microgrid, which was covered by a carbon-coated colodion film and supported by a Cu grid, was used as a substrate for TEM observation. The samples were exposed in air for transportation and observed with the Hitachi HF-2000 TEM operating at 200 kV.

## 3. Results

Figures 2(a), (b), and (c) show typical bright-field (BF) TEM images of the Cr clusters obtained at several $O_2$ gas flow rates, $R_{O_2}$: (a) $R_{O_2} = 0$, (b) $R_{O_2} = 2.2 \times 10^{-7}$ (0.3 sccm), and (c) $R_{O_2} = 7.5 \times 10^{-7}$ mol/s (1.0 sccm), respectively. The experimental parameters were as follows: $L_g = 200$ mm, $R_{Ar} = 2.2 \times 10^{-4}$ mol/s (300 sccm), $R_{He} = 4.5 \times 10^{-4}$ mol/s (600 sccm), and $P_W = 300$ W. Here, $R_{Ar}$ and $R_{He}$ are the gas flow rate of Ar and He, respectively, and $P_W$ is the sputtering power. The corresponding selected-area electron diffraction (SAD) patterns are shown in Figs. 3(a), (b) and (c). At $R_{O_2} = 0$ mol/s, we obtained almost spherical clusters whose sizes are widely distributed between 2 and 20 nm in diameter. The SAD pattern of these Cr clusters displays one set of diffraction rings being ascribed to an A15-type structure with the lattice parameter of $0.46 \pm 0.01$ nm. This is consistent with the reported value of 0.4588 nm.[15] At $R_{O_2} \neq 0$ mol/s, the average cluster size is reduced, being about 5 nm at $R_{O_2} = 7.5 \times 10^{-7}$ mol/s, where the A15-type diffraction rings cannot be detected and the bcc diffraction rings become predominant. Moreover, strong diffraction rings appear inside the (110) ring of the bcc Cr, being ascribed to the (104) and (110) planes of $Cr_2O_3$. The lattice spacings of the (110) plane in bcc Cr, and the (104) and (110) planes in $Cr_2O_3$ are 0.20, 0.24 and 0.26 nm, respectively.

Figures 4(a) and (b) show high resolution TEM images of the typical A15- and bcc-type Cr clusters prepared at $R_{O_2} = 0$ and $2.2 \times 10^{-7}$ mol/s (0.3 sccm), respectively. In Fig. 4(a), the spherical cluster of 17 nm in diameter is viewed along the [021] crystallographic axis. The lattice fringes have a twofold symmetry with the spacing of 0.22 nm, being interpreted to be the (200) lattice planes of the A15 structure. Multi-slice calculation of the above zone axis image contrast of A15-type structure was carried out by MacTempas software (Total Resolution Inc.) for different thickness and defocus values. The observed image agrees well with the one simulated for the thickness, $t = 17$ nm, and the defocus, $\Delta f = -50$ nm. In Fig. 4(b), the cubic shape cluster with the faceted surfaces is observed. The lattice fringes viewed along the [001] axis have a fourfold symmetry, being interpreted to be the (110) and (100) lattice planes of the bcc structure: the observed inter-fringe-distances are 0.19 and 0.27 nm, respectively.

Figure 5 shows a sequence of TOF mass abundance spectra of Cr clusters prepared at several values of $R_{O_2}$. At $R_{O_2} = 0$ mol/s, the TOF signal is very weak and the mass distribution is very broad. With increasing $R_{O_2}$, the mass spectrum of the Cr clusters shifts toward the small size direction and the signal intensity becomes stronger. The deposition rate measured by the thickness monitor also increases with increasing $R_{O_2}$, as shown in Fig. 6.

## 4. Discussion

As shown in the previous section, we have reconfirmed that the metastable A15 phase is formed in the Cr clusters prepared in pure inert gas atmosphere. In small transition metal and inert gas atom clusters, icosahedon-based units have been often observed and assigned as magic numbers.[22] It has been discussed that the stability of such locally close-packed structure units stems from the energy gain of the locally high coordination and the low surface energy.[23] We have also observed the structure change from A15 to bcc by mixing $O_2$ gas with the inert gases in the source chamber and the cluster size variation from 15 to 5 nm with increasing $R_{O_2}$. Since $O_2$ gas reacts with Cr vapor atoms to form $Cr_2O_3$ in the source chamber, it can influence the structural stability.[24] The following mechanisms can be proposed for the present structure change: 1) the formation of $Cr_2O_3$ plays nucleation sites of the bcc phase and 2) the excess heat generated by the $Cr_2O_3$

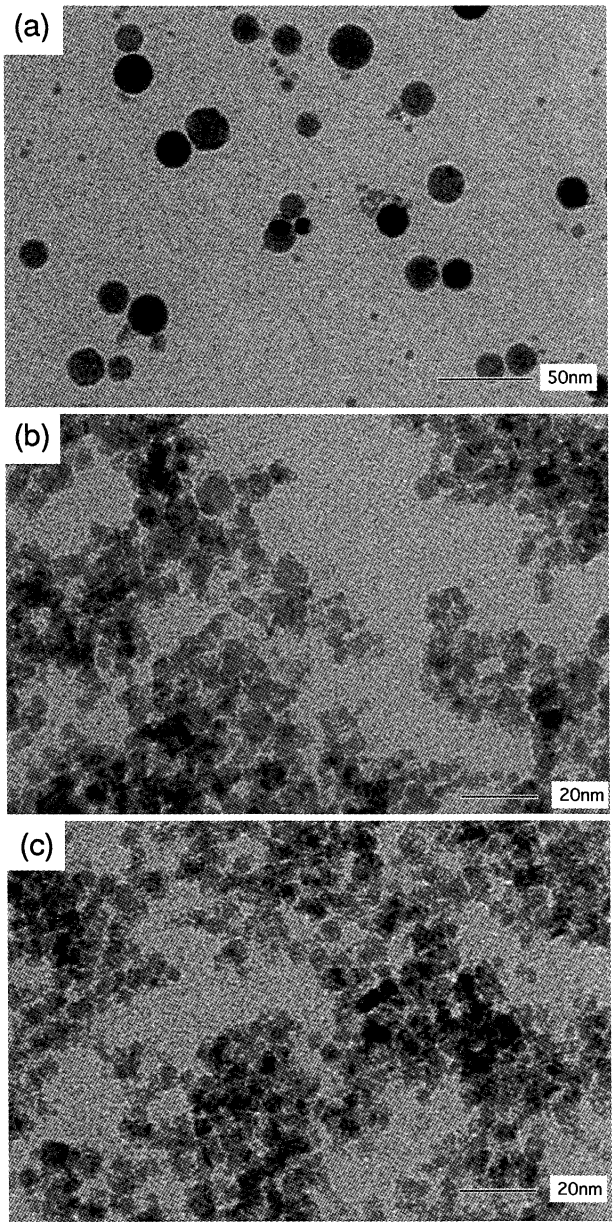


Fig. 2 TEM images for the Cr clusters obtained with different $O_2$-gas flow rate, $R_{O_2}$. (a) $R_{O_2} = 0$, (b) $R_{O_2} = 2.2 \times 10^{-7}$, and (c) $R_{O_2} = 7.5 \times 10^{-7}$ mol/s (1.0 sccm).

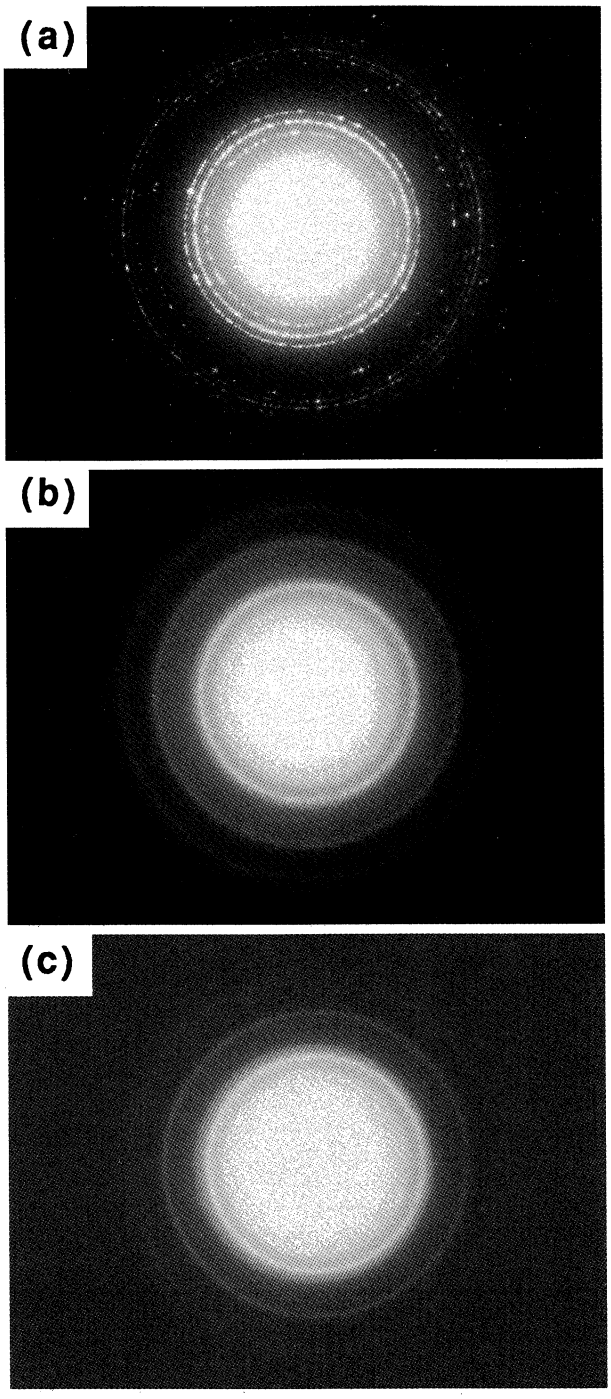


Fig. 3 The SAD patterns corresponding to Fig. 1 for the Cr clusters obtained with different $O_2$-gas flow rate, $R_{O_2}$. (a) $R_{O_2} = 0$, (b) $R_{O_2} = 2.2 \times 10^{-7}$, and (c) $R_{O_2} = 7.5 \times 10^{-7}$ mol/s (1.0 sccm).

formation induces the phase transformation.

Although the sputtering yield drops markedly above the threshold of $O_2$ partial pressure, $p_{O_2}$ (about $10^{-3}$–$10^{-1}$ Pa), it is not so sensitive to $p_{O_2}$ within a small amount of $O_2$ gas addition,[25,26] as the present experiment. Nevertheless, the deposition rate increased dramatically with introducing $O_2$ gas into the cluster source (see Fig. 6). According to the nucleation theory, a heterogeneous nucleation rate is higher than a homogeneous one: the Gibbs free energy of the former is lower than that of the latter, because of smaller surface energy loss in the former. Since the formation enthalpy of $Cr_2O_3$ is negative and its absolute value is rather large, $Cr_2O_3$ molecules and clusters are highly producible and they act as a nucleation site. The more the nuclei, the smaller the cluster size, when vaporized metal atoms are quickly consumed at the cluster's neighbor and the clusters formed are rapidly extracted from the source chamber to the intermediate chamber with the better vacuum condition. This is what we observed by the thickness monitor, TEM, and TOF-MS: the mean cluster size decreased and the deposition rate increased when the $O_2$ gas was introduced into the source chamber.

Cr cluster prepared by the inert gas-deposition method has been systematically reported by Uyeda *et al.*[18] The size of Cr clusters accumulated from the inner zone (the higher temperature region) of the metal smoke was smaller than that from the outer zone (the lower temperature region). The Cr clusters formed at the low temperature region are rapidly quenched to become the metastable A-15 phase, while those formed

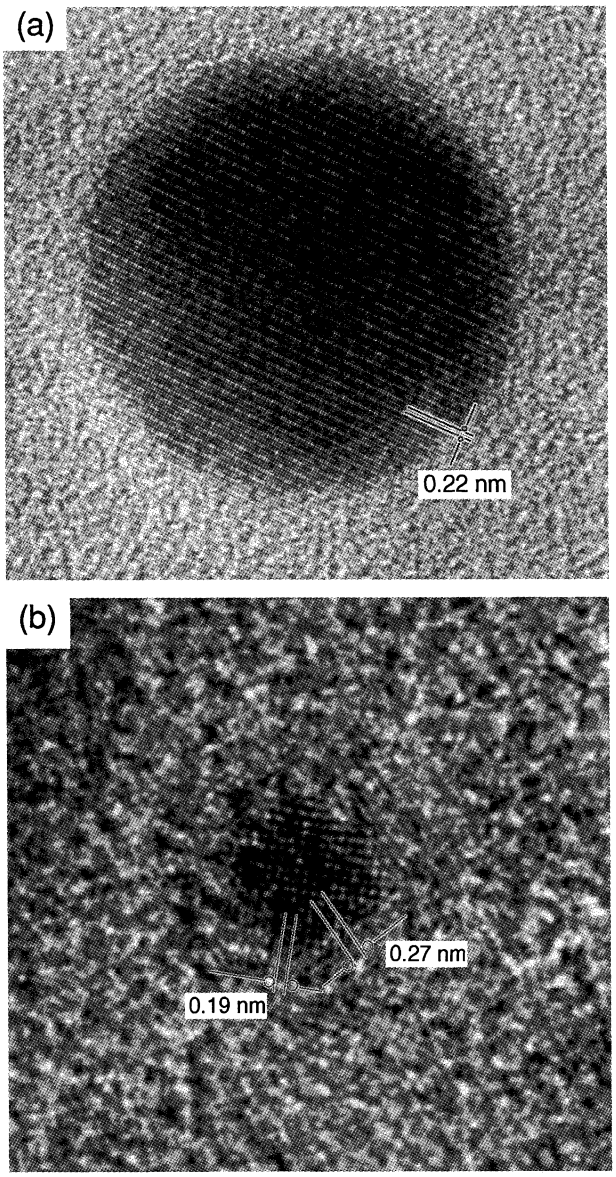


Fig. 4 High resolution TEM images of the typical Cr clusters with (a) A15-type and (b) bcc crystal structure. These clusters were obtained with the different $O_2$-gas flow rate, $R_{O_2}$. (a) $R_{O_2} = 0$ and (b) $R_{O_2} = 2.2 \times 10^{-7}$ mol/s (0.3 sccm).

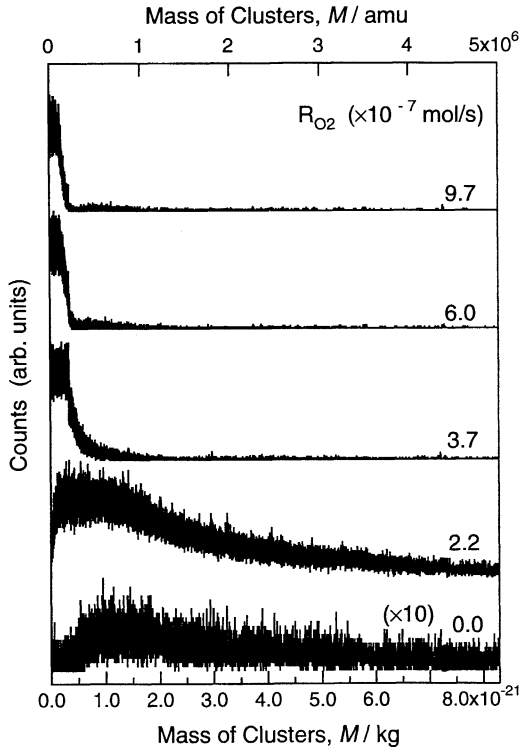


Fig. 5 Mass spectra sequence of the Cr clusters obtained with the different $O_2$-gas flow rate, $R_{O_2} = 0 \sim 9.7 \times 10^{-7}$ mol/s (1.3 sccm).

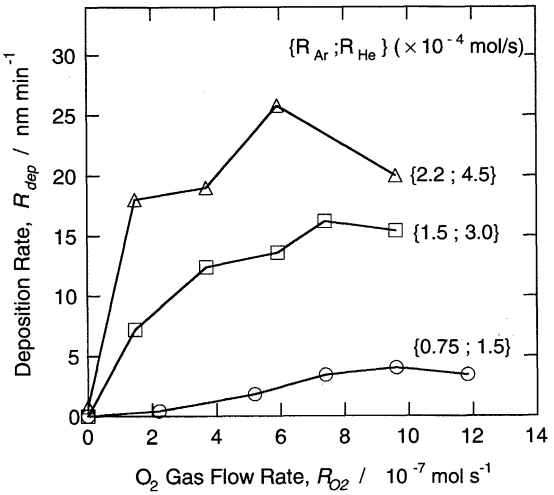


Fig. 6 Deposition rate of the Cr clusters as a function of $O_2$-gas flow rate, $R_{O_2}$.

at the high temperature region are annealed to become the equilibrium bcc phase. These results clearly suggest that the cluster growing processes depend on the ambient temperature. When Cr-atoms and -clusters react with $O_2$ gas, the internal energy of clusters increases and the heat of reaction is released. In order to get an evidence of such heat release, we measured the inert gas temperature, $T(z)$, by putting the alumel-chromel thermocouple attached to the small copper plate ($5 \times 5 \times 1\,\mathrm{mm}^3$) into the source chamber. Figure 7 shows $T(z)$ as a function of the distance from the sputtering target along the beam axis, $z$. $T(z)$ decreases with increasing $z$, because vaporized Cr atoms from the target rapidly loose their kinetic energy by collisions with the inert gas atoms and the thermal radiation effect of plasma is decreased with increasing $z$. At $z < 100$ mm, the temperature difference between $R_{O_2} = 0$ and $R_{O_2} = 7.5 \times 10^{-7}$ mol/s was about 30 K. This temperature rise with $O_2$ gas introduction probably originates from release of the formation enthalpy of $Cr_2O_3$, about 5.9 eV/Cr-atom at 298 K.[27] It probably influences the cluster growth mode, even though the clusters are cooled via collision with He and/or Ar atoms. The energy transfer by a collision between a hot metal cluster and a cold He atom can be estimated to be about $10^{-2}$ eV.[28] It may be effective enough to cool the cluster temperature through such collision events. For the present experimental condition, however, a collision interval between a small cluster and inert gas is about 50 to 500 ns, being longer than the typical phase transformation time of a few ps order estimated from the molecular dynamics calculation.[29] Such small clusters can travel from one potential minimum to another before they are cooled by the collision with inert gas atoms. Hence, it is plausible that the A15 type Cr cluster is heated and transforms to the bcc one when

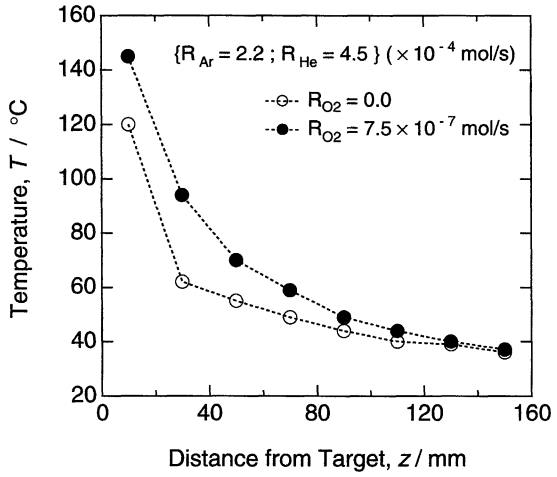


Fig. 7 Inert gas temperature in the PGC cluster source as a function of the distance from target, $z$.

it reacts with $O_2$.

## 5. Conclusion

Nanometric Cr clusters have been fabricated using the plasma-gas-condensation method, and studied by the time-of-flight mass spectrometer (TOF-MS) and transmission electron microscope (TEM). For the Cr clusters prepared in pure inert gas atmosphere, the A15 phase is obtained as a metastable phase. It changes to the bcc phase by introducing $O_2$ gas into the source chamber. The cluster size decreases and the deposition rate increases as the $O_2$ gas flow rate is increased. Moreover, the inert gas temperature in the source chamber increases with $O_2$ gas addition. These results suggest that oxide molecules promote the heterogeneous cluster nucleation, whereas the cluster growth is restricted because of the low density Cr vapor. The exothermic heat also results in the transformation from the metastable A15 to stable bcc phase.

## Acknowledgments

The authors wish to thank Dr. T. J. Konno for useful discussion. This work was supported by CREST (Core Research for Evolution Science and Technology) of Japan Science and Technology Corporation (JST), and a Grant-in-Aid for Scientific Research (11450234) given by the Ministry of Education, Science Culture and Sports of Japan.

## REFERENCES

1) W. A. de Heer: Rev. Mod. Phys. **65** (1993) 611–676.
2) H. Haberland: *Clusters of Atoms and Molecules I and II*, (Springer-Verlag, Berlin, 1995) pp. 207–252.
3) T. P. Martin and T. Bergmann: J. Chem. Phys. **90** (1989) 6664–6667.
4) P. Milani and W. A. de Heer: Rev. Sci. Instrum. **61** (1990) 1835–1838.
5) H. Haberland, M. Karrais, M. Mall and Y. Thurner: J. Vac. Sci. Technol. A **10** (1992) 3266–3271.
6) H. Haberland, M. Mall, M. Moseler, Y. Qiang, T. Reiners and Y. Thurner: J. Vac. Sci. Technol. A **12** (1994) 2925–2930.
7) M. T. Reetz and W. Helbig: J. Amer. Chem. Soc. **116** (1994) 7401–7402.
8) R. L. Whetten, J. T. Khoury, M. M. Alvarez, S. Murthy, I. Vezmar, Z. L. Wang, P. W. Stephens, C. L. Cleveland, W. D. Luedtke and U. Landman: Adv. Mater. **8** (1996) 428–433.
9) A. S. Edelstein and R. C. Cammarata: *Nanomaterials: Synthesis, Properties and Applications*, (Institute of Physics Publishing, Bristol and Philadelphia, 1996) pp. 303–436.
10) P. Melinon, V. Paillard, V. Dupuis, A. Perez, P. Jensen, A. Hoareau, J. P. Perez, J. Tuaillon, M. Broyer, J. L. Vialle, M. Pellarin, B. Baguenard and J. Lerme: Int. J. Mod. Phys. B **9** (1995) 339–397.
11) G. Hohl, T. Hihara, M. Sakurai, T. J. Konno, K. Sumiyama, F. Hensel and K. Suzuki: Appl. Phys. Lett. **66** (1995) 385–387.
12) S. Yamamuro, K. Sumiyama, M. Sakurai and K. Suzuki: Supramol. Sci. **5** (1998) 239–245.
13) S. Yamamuro, K. Sumiyama and K. Suzuki: J. Appl. Phys. **85** (1999) 483–489.
14) T. Hihara and K. Sumiyama: J. Appl. Phys. **84** (1998) 5270–5276.
15) T. Hihara and K. Sumiyama: J. Vac. Sci. Technol. B **17** (1999) 1923–1929.
16) K. Kimoto and I. Nishida: J. Phys. Soc. Jpn. **22** (1967) 744–756.
17) C. J. Doherty, J. M. Poate and R. J. H. Voorhoeve: J. Appl. Phys. **48** (1977) 2050–2054.
18) Y. Saito, K. Mihama and R. Uyeda: Jpn. J. Appl. Phys. **19** (1980) 1603–1610.
19) T. Onozawa and K. Takayanagi: Surf. Sci. **357–358** (1996) 228–232.
20) J. P. Chu, J. W. Chang, P. Y. Lee, J. K. Wu and J. Y. Wang: Thin Solid Films **312** (1998) 78–85.
21) M. Arita and I. Nishida: Jpn. J. Appl. Phys. **32** (1993) 1759–1764.
22) M. Sakurai, K. Watanabe, K. Sumiyama and K. Suzuki: J. Chem. Phys. **111** (1999) 235–238.
23) S. Sugano: *Microcluster Physics: Series in Materials Scinece 20*, (Springer-Verlag, Berlin, 1991) pp. 1–15.
24) C. G. Granqvist and R. A. Buhrman: J. Appl. Phys. **47** (1976) 2200–2219.
25) J. Heller: Thin Solid Films **17** (1973) 163–176.
26) T. Abe and T. Yamashina: Thin Solid Films **30** (1975) 19–27.
27) F. R. de Boer, R. Boom, W. C. M. Mattens, A. R. Miedema and A. K. Niesen: *Cohesion in Metals*, (Elsevier Science, Amsterdam, 1988) pp. 751–754.
28) J. Troe: J. Chem. Phys. **66** (1977) 4758–4775.
29) T. L. Beck, J. Jelius and R. S. Berry: J. Chem. Phys. **87** (1987) 545–554.